Micromachined Antenna Stents and Cuffs for Monitoring Intraluminal Pressure and Flow

Kenichi Takahata, *Member, IEEE*, Yogesh B. Gianchandani, *Senior Member, IEEE*, and Kensall D. Wise, *Fellow, IEEE*

***Abstract*—This paper describes two stainless steel microstructures that are microelectrodischarge machined from 50-μm-thick planar foil for intraluminal measurements of pressure and flow (with potential for applications ranging from blood vessels to bile ducts). The first structure is an inductive antenna stent (stentenna) with 20-mm length and 3.5-mm expanded diameter. It is coupled with capacitive elements to form resonant *LC* tanks that can be telemetrically queried. The resulting *LC* tanks are deployed inside silicone mock arteries using standard angioplasty balloons and used in a passive telemetry scheme to sense changes in pressure and flow. Using water as the test fluid, the resonant peaks shift from about 215 to 208 MHz as the flow is increased from 0 to 370 mL/min. The second structure is a ring-shaped intraluminal cuff with two 400×750-$\mu\mathrm{m}^2$ electrodes that are used to provide a direct transduction of flow velocity in the presence of a magnetic field. It is fabricated in a manner similar to the stentenna, but with an insulating segment. The voltage has a linear dependence on flow rate, changing by 3.1–4.3 μV per cm/s of flow (of saline) over a 180 cm/s dynamic range, with a magnetic field of about 0.25 T. [1733]**

***Index Terms*—Bloodflow, cardiac, microelectrodischarge machining, sensor network, wireless.**

I. Introduction

In recent years, stents have come to play an essential role in the treatment of cardiovascular and other diseases. Most commonly implanted in the coronary artery, the cardiac stent typically has mesh-like walls in a tubular shape, and once positioned by a catheter, is expanded radially by the inflation of an angioplasty balloon. Its primary task is to physically expand and scaffold blood vessels that have been narrowed by plaque accumulation. However, renarrowing (restenosis) often occurs due to blood clot (thrombus) formation, excess growth of intravascular tissues (proliferation), and further plaque deposition [1]. While the availability of drug-eluting stents can suppress these failures in certain cases, chronic monitoring of pressure or flow is still needed in others. Another category of vascular problems in which stents are used is aortic aneurysms, which may be thoracic or abdominal. Such aneurysms have been surgically treated in the past, but the use of stents for this purpose is increasing [2], [3]. While use of wireless pressure sensors has been reported in association with these stents [4], the sensors are located in the aneurysm, not within the stent or path of blood flow. For this reason, miniaturization is not essential, and sensors of 1–2 cm length can be accommodated. Stents are also used in the carotid artery [5], bile duct [6], pancreatic duct [7], tracheobronchial airways [8], and in the esophagus [9] to treat diseases ranging from atherosclerosis to carcinoma. Since their intent is inevitably to facilitate the movement of some kind of fluid, the innate ability to monitor intraluminal pressure or flow can provide advance notice of the need for further tests or intervention.

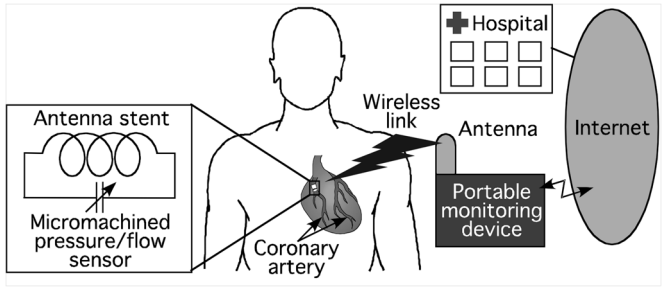

Fig. 1. A wireless link to an implanted sensor can be monitored by a portable device placed in the residence or on the person of the patient. This can then provide a link to a database through the internet or a broader wireless network, permitting physicians to review the sensed parameters.

For many applications, the absolute value of pressure and flow is not required; a simple change in the average or instantaneous signal over time can provide a warning to be heeded by a more direct and precise diagnosis. This eases the burden of functional performance on the implanted device, and opens up some options for engineering simpler solutions.

The use of wireless telemetry can alleviate a lot of the practical challenges associated with monitoring implanted sensors. For example, pressure can be monitored using a microchip that has a planar thin film inductor integrated with a micromachined capacitive pressure sensor [10]–[14]. This *LC* tank circuit couples to a separate external transmitting coil via mutual inductance, responding to a change in pressure by a shift in the frequency at which the external coil shows a characteristic dip in impedance or phase. If a stent is able to serve as an inductor/antenna and is integrated with microsensors, the planar inductor can be eliminated from the *LC* tank (saving considerable space), and the stent can become an inherent element in the wireless link (Fig. 1).

Manuscript received December 11, 2005; revised February 20, 2006. The exploration of microdischarge based process methods was supported in part by a Grant from the National Science Foundation. The design and fabrication of the pressure sensors was supported by the Engineering Research Centers Program of the National Science Foundation under Award Number EEC-9986866. Subject Editor S. Shoji.

K. Takahata was with the Department of Electrical Engineering and Computer Science, University of Michigan, Ann Arbor, MI 48109 USA. He is now with the University of British Columbia, Vancouver, BC V6T 1Z4, Canada (e-mail: takahata@ece.ubc.ca).

Y. B. Gianchandani and K. D. Wise are with the Department of Electrical Engineering and Computer Science, University of Michigan, Ann Arbor, MI 48109 USA (e-mail: yogesh@umich.edu; wise@umich.edu).

Digital Object Identifier 10.1109/JMEMS.2006.880229

While most commercially available vascular stents are made by laser machining of stainless steel tubes, other constructions—such as threaded wire structures, or rings made from shape-memory alloy and sutured to woven polyester—are also used [3], [15]. It has been recently shown that stents cut from planar metal foils by microelectrodischarge machining (μEDM) offer appropriate mechanical properties [16]. These stents use flexural designs and do not have any bonded or welded seams. In assembling the device, a deflated angioplasty balloon is threaded alternately above and below a series of involute cross bands that lie between two longitudinal side beams, and then expanded by a normal angioplasty procedure. This design approach permits stents to be fabricated from steel foil by using planar electrodes as "cookie cutters" that are lithographically fabricated on a silicon substrate [17]. It also offers compatibility with other planar microfabrication processes based on lithographic techniques. While the stents reported in [16] were simply mechanical devices, it was recognized that inductive coils could also be fabricated in this way.

This paper explores the possible use of stent-like structures micromachined from planar foils for chronic monitoring of intraluminal conditions within an artery, duct, fistula, or other flow path.[1] Two complementary approaches are investigated. The first one, described in Section II, explores a structure that integrates silicon-micromachined capacitive pressure sensors with a dual-inductor stentenna to form a device for wireless flow measurement. The second approach, described in Section III, explores structures for the electromagnetic (EM) detection of flow [22], [23] in a polarizable liquid. Section IV addresses some of the ways that performance may be improved in particular applications, whereas Section V draws conclusions from the overall effort.

II. A Dual-Inductor Stentenna With Two Pressure Sensors

When a liquid flows through a channel, there is a pressure drop between two separate locations that depends on the flow rate. A general expression for this drop in steady-state flow is [24]

$$P_2 - P_1 = R_a V + R_b V^2 \tag{1}$$

where P_1 and P_2 are pressures at downstream and upstream locations, respectively, V is area-averaged flow velocity in an unobstructed vessel, and R_a and R_b are coefficients that depend on obstacle geometry and fluid properties. The first term is associated with a loss due to viscous shearing stress, and the second is due to geometry variation inside a channel, such as by redeposited plaque or excess tissue growth over a stent. As the obstruction grows, the nonlinear term tends to dominate. With a correction for average pressure, changes in the local pressure at a site (that has been strategically selected for chronic monitoring) can provide indication of an impending medical problem. Further, if there are two pressure sensors that are located upstream and downstream of a blockage, they can be used differentially to determine the absolute flow, and a separate measurement of average pressure is not needed. However, if the two pressure sensors are not used differentially but are instead used to provide a single averaged reading, their output can be indicative of changes in flow due to blockages that are upstream or downstream of both of them.

[1]Portions of this manuscript have been presented in conference abstract form in [18]–[21].

A. Stentenna Design

For an effective wireless link, minimal damping is desired in the *LC* tank (Fig. 1). The quality factor, Q, is expressed as

$$Q \approx \frac{1}{R_{STp}} \sqrt{\frac{L_{ST}}{C_{SE} + C_{STp}}} \tag{2}$$

where L_{ST} is inductance of the stentenna, C_{SE} is capacitance of the sensor, C_{STp} is parasitic capacitance, and R_{STp} is parasitic resistance. The impact of the R_{STp} is greater than that of C_{STp}. For a given material, and at frequencies low enough that the skin effect is not a factor, the parasitic resistance of the stentenna is inversely related to the cross sectional area of its beams. However, the parasitic capacitance that it contributes is proportional to the beam surface area. Therefore, R_{STp} depends on the square of the beam diameter whereas C_{STp} is simply proportional to it. Thus, it can be electrically favorable to increase the thickness of the beams. In fact, this is favorable mechanically as well, because it would increase the radial stiffness of the stent. However, from the biological viewpoint, increasing the volume of the structural elements can be undesirable, and may warrant application-specific designs and structural optimization. In this effort the stentennas had beams of 50×50 μm^2 cross section. This is similar to the purely mechanical stents reported in [16], and at the lower end of the range offered in existing commercial options.

The planar microstructure that was used in this effort is illustrated in Fig. 2(a). It has a series of cross bands that have involute contours with a bridge to a longitudinal beam at the center of the device. The involute bands form dual inductors, whereas the beam is a common electrical node. At each end of the device the bands terminate in a section that forms a ring. This provides enhanced mechanical rigidity in the pre-expansion state as the angioplasty balloon is inserted into it. It also provides improved radial stiffness after expansion. Capacitive pressure sensors are connected across the common line and a lead that is connected to the ring, thereby implementing two *LC* tanks when complete.

During the deployment of a stent, the structure is pushed against the walls of the lumen as the angioplasty balloon is inflated, so it is necessary to consider the immunity of the micromachined pressure sensors from overpressure in this step. While capacitive pressure sensors have natural overpressure protection because the diaphragm deflection is constrained by the substrate, the range of pressures used in balloon angioplasty (4–12 atm.) can still be of some concern. Having platforms for the sensors in the stentenna structure not only permits rigid bonding of the pressure sensors, but also helps to protect them during balloon inflation. Several preliminary experiments were conducted with dummy samples that were pressurized by balloons inside 3-mm i.d. silicone mock arteries with 0.25-mm-thick walls, which are manufactured for the purpose

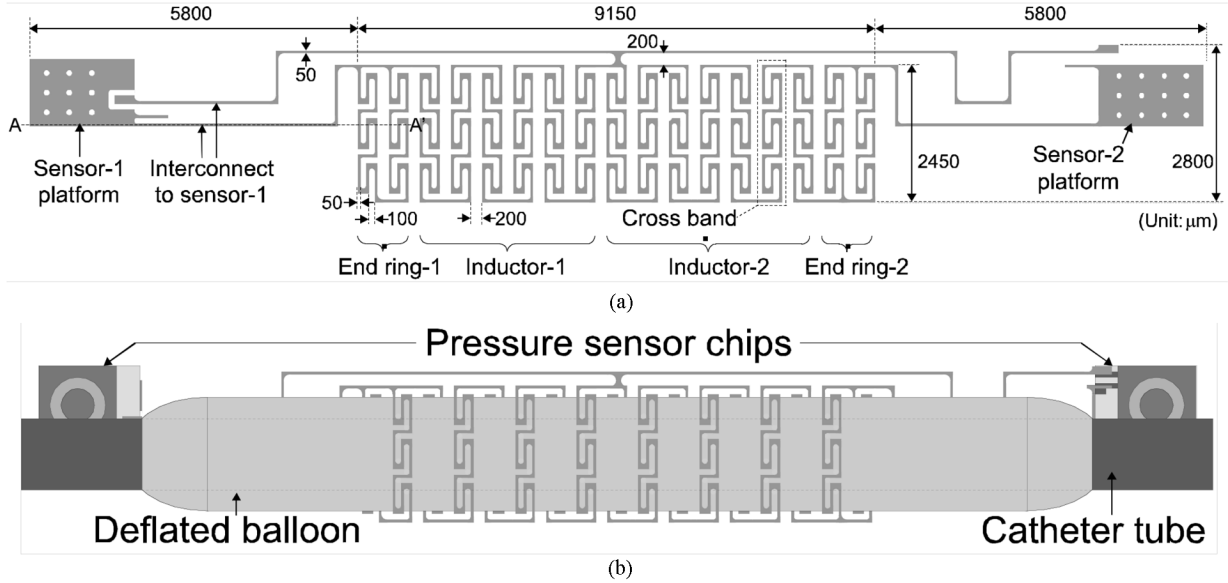

Fig. 2. (a) Stentenna design for μEDM patterning. (b) A stentenna integrated with two sensor chips is mounted on a deflated angioplasty balloon.

of testing vascular implants and have compliance similar to human arteries (Dynatek Dalta Scientific Instruments, MO) [25]. They showed, in fact, that the sensors had no damage and were still functioning even after full expansion of the stent to 3.5-mm diameter. However, to provide an extra measure of security, as shown in Fig. 2(b), the stent was designed to locate the sensors outside the longitudinal span of the balloon, which had a 16-mm length in this case.

B. Device Fabrication

Although stents that serve purely mechanical purposes do not require any insulation, the stentenna plays an electrical role and does require insulation from the surrounding fluid. Electrical isolation is particularly needed between the cross bands of the stentenna that might otherwise contact each other and shunt out the inductance if the angioplasty balloon expands nonuniformly. Further, this insulation should cover the micromachined pressure sensors and lead transfers to them, and be biocompatible as well. Parylene-C was chosen as the coating material because it provides a thin, uniform and conformal coating that is nonconductive, chemically inert, and biocompatible. It also has a history of applications to biomedical devices, including cardiac stents [26].

The majority of commercial stainless-steel stents use type 316L steel. This differs from type 304, which is one of the most common and versatile grades of steel. Type 316 steel has molybdenum (2%–3%), which gives it better overall corrosion resistance than 304; type 316L is a low carbon version of 316, which is immune to carbide precipitation at grain boundaries. However, a comparison of the important material properties of these three kinds of steel (Table I) shows that for *in vitro* tests, they have very similar characteristics. Consequently, in this effort 304 steel was used because it was easily available in 50 μm thick foils.

Fig. 3 shows the process flow using a cross-sectional view at A-A' in Fig. 2(a). First, the steel foil is patterned by μEDM (step "a"). The machined structure remains connected to the original sheet at this point for ease of handling during subsequent steps. Pressure sensors fabricated on a 500-μm-thick glass substrate are diced into 1.4×1.8 mm^2 chips in advance. Two sensors are attached to platforms which are linked at the ends of the longitudinal beams extended from the rings (step "b"). The bonding is performed with enamel, which offers good adhesion and mechanical strength, and it is also easily applied and cured rapidly. Perforations in the platforms serve as escape paths for excess enamel. The sensors are then electrically connected to the leads

TABLE I
COMPARISON OF SELECTED PROPERTIES BETWEEN TYPE 304 AND 316L STAINLESS STEELS [27], [28]

	Young's modulus (GPa)	Ultimate stress (MPa)	Hardness (Rockwell B)	Electrical resistivity ($10^{-5}\Omega$·cm)	Magnetic permeability	Density (kg/m3)
304	193	580	80	7.2	1.008	8000
316L	193	560	79	7.4	1.008	8000

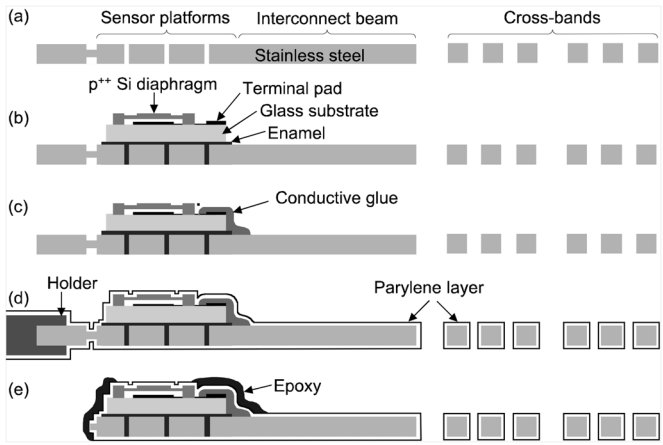

Fig. 3. Fabrication flow. (a) μEDM stainless steel foil. (b) Glue down sensor chips. (c) Electrically connect to terminal pads of the sensors. (d) Deposit passivation layer. (e) Release device and apply epoxy to the perimeter of the sensors.

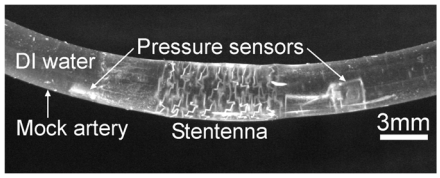

(a)

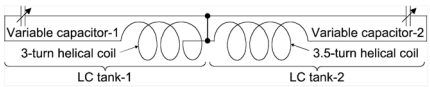

(b)

Fig. 4. (a) Deployed device with balloon removed. (b) Equivalent circuit after expansion completed.

with a conductive adhesive (step "c"). The device is next coated with 0.5-μm-thick parylene everywhere for electrical insulation (step "d"). Since this is a vapor-phase deposition step, the coating is conformal. The device is then mechanically released from the sheet (step "e"). Finally, additional epoxy is applied to the perimeter of the sensors to enhance the bonding strength.

The micromachined pressure sensor consists of a vacuum-sealed cavity capped by a 3.7-μm-thick p^{++} silicon circular diaphragm with a 1-mm diameter and 5-μm gap [29]. The diaphragm has a 10-μm-thick boss for better linearity and an oxide layer on the backside for electrical protection in case of contact between the diaphragm and a bottom electrode, which is a thin film of Ti/Pt/Au patterned on a 500-μm-thick Pyrex glass substrate. In the experiments described here, the glass substrate of a pressure sensor that is upstream of the stentenna was thinned (by wet etching) down to 100 μm in order to create a more streamlined profile. Of course, this can be done to the other pressure sensor as well.

The fabricated devices are then deployed inside a mock artery using a standard angioplasty balloon with a 3.5-mm inflated diameter. In this step, the stentenna becomes permanently deformed from a planar into a helical shape, which consists of two separate coils with 3 and 3.5 turns in this case (Fig. 4). As noted previously, the two sensors are located just off the region occupied by the balloon, minimizing the physical impact to both the sensors and the tube wall.

C. Experimental Setup and Results

Fig. 5 shows the fluidic test setup used to evaluate the device in Fig. 4. A pump/flow-controller regulates the flow (of water), and a separate meter (PS309, Validyne Engineering Co., CA) measures the differential pressure drop along the 8-cm-long tube. To simulate a blockage, a dielectric rod with 1.5-mm diameter is positioned inside the stentenna. The complex input impedance of an external coil is monitored with an HP4195 spectrum analyzer. The output power fed from the analyzer to the external coil is $\approx$ 1 mW, which makes the power density well below a biological threshold of 10 $\mathrm{mW/cm^2}$ recommended by ANSI for the purpose of protecting human health [30]. The stentenna inductance is approximately 110 nH in total. The pressure sensors have a measured response of ≈ 6 fF/torr [see Fig. 6(a)], which reduces to $\approx$ 2 fF/torr with a 1.3-μm -thick parylene coating. Sensor 1, which has lower capacitance,

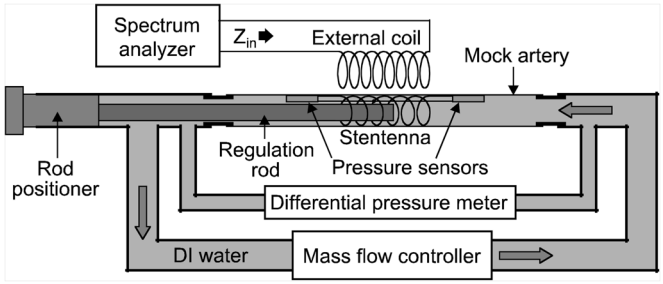

Fig. 5. A setup for wireless pressure/flow sensing.

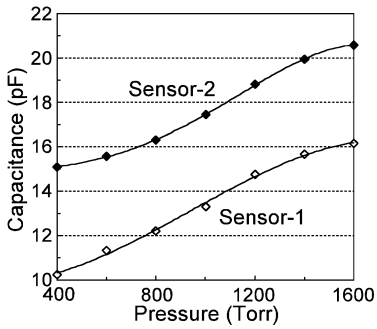

(a)

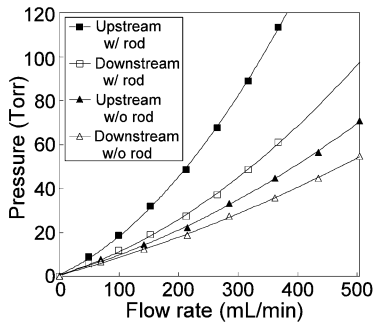

(b)

Fig. 6. (a) Measured response of uncoated capacitive pressure sensors. (b) Measured gauge pressure versus flow rate with and without the regulation rod that serves as a partial obstruction to the flow.

is coupled to the 3-turn inductor, and sensor 2 is paired with the 3.5-turn inductor, so that these *LC* tanks have different resonant frequencies. If the quality factor of these resonant tanks was sufficiently high, they would produce discernible peaks yielding the upstream and downstream pressures separately. However, the present implementation offers relatively low inductance due to limitations in machining resolution, which means that the peaks will be merged together.

Fig. 6(b) shows gauge pressure at upstream and downstream locations as a function of flow rate, which is measured with the setup of Fig. 5. The plot also shows its dependence on the obstruction, which causes a quadratic dependence on flow rate that is consistent with (1). The nonlinearity in the curve for unobstructed flow (i.e., no rod) comes from the flow resistance of the device itself.

An impedance peak that is nominally at 239.1 MHz in a 4-mm diameter external coil with inductance of 610 nH is shifted down by increasing flow rate as shown in Fig. 7(a). Fig. 7(b) plots this frequency shift and the corresponding differential pressure

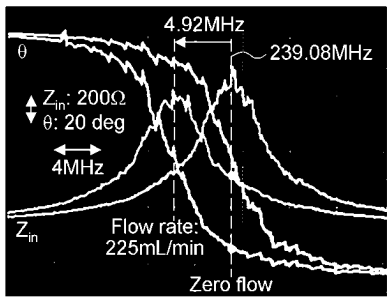

(a)

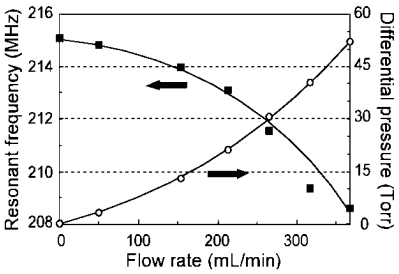

(b)

Fig. 7. (a) Measured amplitude of input impedance Z_{in} in an external coil shifted near 239 MHz due to flow change. (b) Measured resonant frequency and differential pressure versus flow rate.

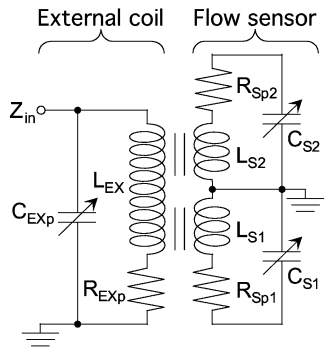

Fig. 8. A possible model for the microsensor system.

drop: there is a reduction of 9–31 KHz per mL/min. increase in the flow range over 370 mL/min. (Typical coronary artery flow is 100–200 mL/min.) The pressure response observed is 57.4 KHz/torr (at gauge pressure of 113 torr), while the corresponding sensitivity is 273 ppm/torr. These preliminary measurements were taken in close proximity, with the receiving coil < 1 cm away from the stentenna.

Fig. 8 shows a qualitative model for the wireless setup in Fig. 5. In this model, L_{EX}, L_{S1}, L_{S2}, C_{S1}, and C_{S2}, respectively, denote inductance of an external coil, inductance for the downstream inductor, that for the upstream inductor, capacitance of sensor 1, and that of sensor-2. The two inductors of the device are mutually coupled to the external coil. It also shows parasitic elements C_{EXp}, R_{EXp}, R_{Sp1}, and R_{Sp2}, which are capacitance for the external coil, resistance for the coil, lumped resistance for the downstream *LC* tank, and that for the upstream tank, respectively. Other parasitics (not shown) include capacitances that are associated with the stentenna, capacitive pressure sensors, and their packaging. While this model is helpful for the qualitative understanding of the device operation, it is quantitatively very sensitive to the values of the parasitic elements as well as the strength of the wireless coupling between the three inductors, and should be used with caution for predictive modeling.

III. A Cuff for Electromagnetic Flow Measurement

The principle of the electromagnetic flow sensing is based on Faraday's law of magnetic induction. When polarizable liquid passes through a magnetic field at an angle, a voltage is generated across the flow channel, in a manner analogous to the Hall effect. This voltage is sensed by two electrodes that are placed on the channel walls, and is given by [22]

$$V_{EM\_MAX} = D \cdot B \cdot v \cdot \cos\varphi \cdot \cos\theta \tag{3}$$

where D is the diameter of the flow channel, B is the magnetic flux density and v is the cross-sectional average velocity of the flow. In a Cartesian coordinate system, if the flow is parallel to the z axis and the voltage is sensed along the y axis, then the angles θ and φ are, respectively, the angles made by the magnetic field to the x–y and x–z planes. This equation assumes that (a) the magnetic field is spatially uniform, and (b) the flow velocity profile is axially symmetric. The condition (b) is valid downstream of a narrowed site if the location is reasonably distanced from the blockage. The output voltage is independent of conductivity over a wide range [31] (which is preferably $> 5\ \mu\mathrm{S/cm}$), and thus EM sensing is, in principle, widely applicable. It has been used in diverse fields including food, chemicals, paper and pulp, water supply, and energy supply industries [32].

Blood flow measurement has been a major application of EM flow sensors [33]–[40]. A number of devices for blood flow sensing that were based on this detection scheme were developed in late 1960's and early 1970's. Some of these included electromagnetic or permanent magnet elements for the local application of the magnetic field, whereas others relied upon an externally applied one. Additionally, the devices could be perivascular, cannular, or intravascular. The earliest perivascular devices used sense electrodes that were placed external to the lumen. As researchers developed ways to miniaturize the lateral dimensions of devices (in part by relying on an external magnetic field), intravascular designs were developed. Not surprisingly, the devices used three–dimensional (3-D) construction methods, and required the assembly of multiple components made of different materials. In general, they were also intended for acute usage, either because of their relatively large size, or because they were intended to remain at the tip of a catheter that partially occluded the flow path. For chronic implants, of course, it is necessary to insure that fouling of the sense electrodes does not interfere with the measurements.

A drawback of this method is its dependence upon orientation of magnetic field. For example, when the magnetic field is tilted by 15° for both θ and φ, the signal loss is estimated to be 6.7%. This is not necessarily a major problem for every potential application. However, to the extent that correction is needed, one past approach has been to include a calibration sensor and its circuitry within the catheter-based structure [35]. Another used a built-in electromagnet so that a magnetic flux with a fixed orientation is provided to the sensing site [36].

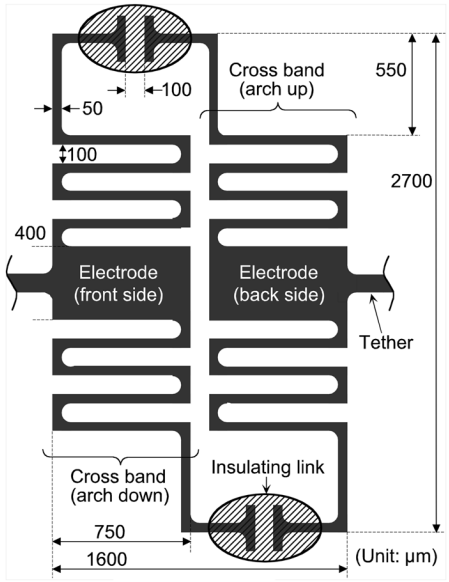

(a)

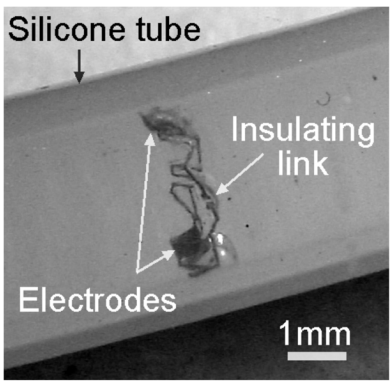

(b)

Fig. 9. (a) A layout of the planar cuff structure. (b) Expanded cuff remains attached to the inner walls of the tube by pressure after the balloon is deflated and removed. (The lead wires have been removed.)

In this part of the effort, flow sensing is facilitated primarily by an intraluminal cuff that senses the EM voltage. Fabricated by a lithography-compatible approach similar to the one described for the stentenna, this structure is conformal to the inner wall of the lumen, and has a low profile. It has two electrodes located diametrically across from each other. These electrodes are electrically insulated from each other by dielectric links formed in the cuff. The voltage built up between the electrodes is sensed by a separate component. While this device is not intended specifically for vascular applications, it is not incompatible with such use.

A. *Fabrication and Testing*

The planar microstructure for the cuff has a pair of meander bands comprised of 50-μm-wide beams, electrode plates ($400 \times 750\ \mu\mathrm{m}^2$), and two dielectric links which mechanically tie the bands but electrically insulate them from each other [Fig. 9(a)]. This pattern is cut by μEDM into 50-μm-thick #304 stainless steel foil so that the two bands are connected to the original foil at tethers shown in Fig. 9(a), maintaining 100-μm

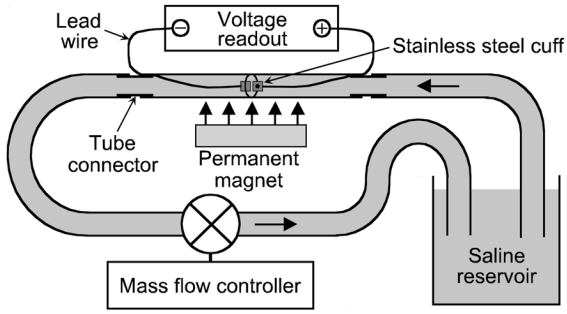

Fig. 10. A setup for the flow measurement with the cuff.

gaps at the links. Insulating cement is used to bridge the gaps, and then the device is released from the foil at the tethers. This is similar to the process flow for a Kelvin probe described in [41]. Lead wires are bonded to the electrodes with conductive adhesive. All surfaces of the device except the front surfaces of the electrodes are coated with an insulating layer. (Without this, spatial averaging could reduce the signal voltage.) The electrode may be optionally coated with an antifouling layer. This feasibility experiment uses two-part epoxy and enamel for the cement and the insulation layer, respectively. The fabricated planar structure is mounted on a deflated angioplasty balloon of a standard angioplasty catheter so that one of the bands is located above the balloon whereas the other band is below it.

The cuffs were tested in silicone tubes with 3-mm i.d. To implant a cuff, the angioplasty balloon was inflated up to 3.5 mm in diameter and then deflated and removed from the tube, leaving the expanded cuff within the tube [see Fig. 9(b)]. Tests with flow velocities up to 2 m/s show that both the structure and its placement are robust and immovable. (As a point of comparison, the maximum arterial flow is typically $\approx 1.6\ \mathrm{m/s}$). The fluidic test setup is shown in Fig. 10. A pump/flow-controller regulated the flow of 2% wt. saline and a voltmeter measured voltage between the electrode leads. A permanent magnet with dimensions of $25 \times 25 \times 9\ \mathrm{mm}^3$ was used to provide magnetic field. The field orientation was perpendicular to both flow direction and the voltage sense axis defined by the locations of the two electrodes. The magnetic field was characterized by an InAs Hall sensor (BH-205, F. W. Bell, FL) and measured as $\approx 0.25\ \mathrm{T}$ at the location of the cuff. The presence of the cuff had no detectable impact on the externally measured magnetic field. A baseline voltage can be associated with polarization and electrochemical effects, so the flow-dependent voltage was measured with opposing orientations of the magnetic field (Fig. 11). The transduction was linear and symmetric, and the voltage response and sensitivity were 3.1–4.3 μV per cm/s and 50–70 ppm per cm/s, respectively.

Using (3) with $D = 3\ \mathrm{mm}$ and $B = 0.25\ \mathrm{T}$, the calculated output voltages are plotted with a dotted line (Cal-1) in Fig. 12(b). Although at low flow velocity the prediction matches well with the experimental result, it deviates as the flow velocity is increased. Fig. 12(a) shows the actual electrode positions observed in the expanded cuff, which are not actually on a diametrical line but are shifted by approximately

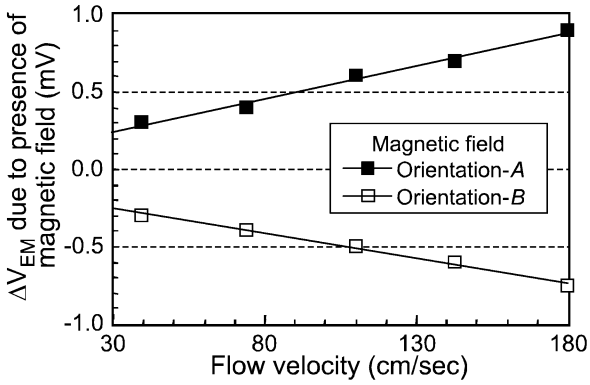

Fig. 11. Measurement result showing linear dependence on flow velocity and symmetric responses with opposing magnetic fields.

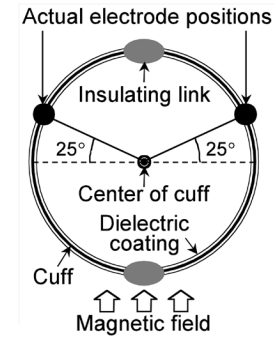

(a)

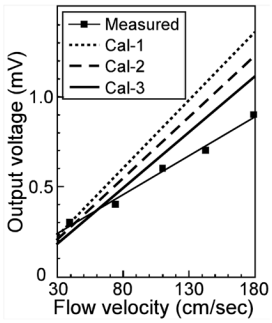

(b)

Fig. 12. (a) Electrode positions in the cuff structure. (b) Measured and projected voltages as a function of flow velocity.

50° in total during the balloon inflation. This nonuniform expansion can lower the output voltage. Two hypothetical cases are evaluated and plotted in Fig. 12(b): in one, each of the electrodes is equally offset by 25° as shown in Fig. 12(a) (Cal-2), while in the other one of the electrodes is offset by the entire 50° (Cal-3). The latter appears to be a better match. A further source of error is the loss associated with the nonideal profile of flow velocity. The presence of electric lead wires, which are connected to the electrodes and/or the cuff itself, can disturb the flow. The sensitivity to local flow velocity varies across the channel and rapidly increases close to the electrodes [42]. Thus, the disturbance near an electrode due to the boundary irregularities can potentially require a correction factor to be introduced into the theoretical estimate, which is otherwise idealized. The use of relatively large electrodes in the setup may have also contributed to the reduced response.

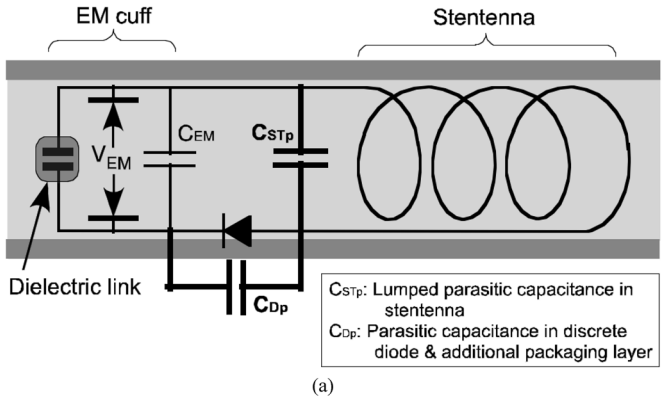

(a)

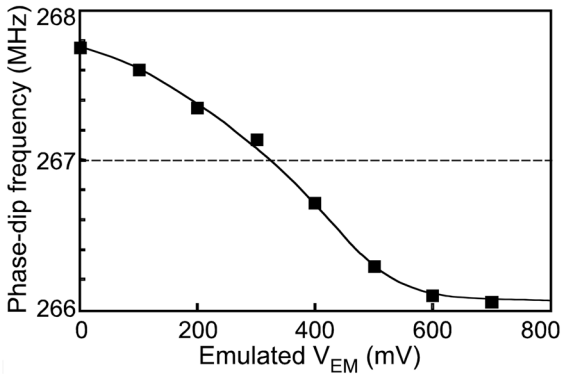

(b)

Fig. 13. (a) Parasitic capacitances in the actual placement of the wireless EM sensor. (b) Measured frequency shift with the emulated V_{EM}.

B. The Wireless Option

For chronic intraluminal monitoring, the EM cuff may be combined with a microelectronic interface chip that is telemetrically powered and controlled. A stentenna that is co-located with it can potentially serve as its wireless link. However, there could be cases in which the size of the chip prevents its use, and a smaller device with reduced functionality would be preferred. One possible way to implement a passive readout of a fully intraluminal EM flow sensor is by combining the inductance of the stentenna and the capacitance of a varactor to form an *LC* tank. In this scheme, the stentenna and the varactor are connected in series, and the ends of the series pair are terminated by the two electrodes of the EM cuff [see Fig. 13(a)]. The varactor is biased by the V_{EM} generated between the electrodes to modulate the resonant frequency of the tank. This circuit is interrogated wirelessly by an inductive coupling between the tank and an external coil, as used for the pressure-based device in Section II.

As a preliminary test, the junction capacitance of a diode (1N3595, Fairchild Semiconductor Co., ME) was used as the varactor. Since the threshold voltage of the diode is much higher than a typical range of V_{EM}, the series-connected tank achieves high input impedance. The stentenna structure was fabricated by patterning a 50-μm-thick stainless steel sheet by μEDM and then electroplating it with copper to reduce the parasitic resistance of the structure and, therefore, increase the quality factor of the tank. The resistance of the stentenna, which was originally 14 Ω, was reduced to about 1/10 of the value with

a 3-μm-thick copper coating. The structure was then coated with 1-μm thick parylene-C, leaving the electrodes exposed. The diode was then mounted on the structure and sealed with insulating epoxy for both electrical and mechanical protection. The assembly was then mounted on a deflated angioplasty balloon and deployed inside a test lumen. An emulated V_{EM} (provided by a power supply) was used to modulate the varactor, while the frequency at which the resonant phase dip occurred was monitored in an external coil. Fig. 13(b) shows the measured response of 2.0–3.3 KHz/mV that saturates as it reaches a turn-on voltage of the diode, which is 680 mV in this case.

The challenge in this architecture lies in finding a varactor with sensitivity that is high enough and parasitics that are low enough that it can be substantially modulated by the voltages built up on the cuff. In particular, it is important for any parasitic shunt capacitance and conductance in the varactor to be as low as possible so as not to load the voltage source. The parasitic capacitances that are particularly detrimental include C_{STp} (which is a lumped equivalent of the parasitic capacitance in the stentenna), and C_{Dp} (which is the parasitic capacitance in the discrete diode) as illustrated in Fig. 13(a).

IV. Discussion

In order to improve performance of the stentenna, one of the priorities is to increase the inductance per unit length. With respect to the pressure-based measurement that was described in Section II, it is noted that a single resonance peak was observed even though two pressure sensors were available. To obtain a differential measurement from these devices, it will be necessary to increase of the quality factor of the *LC* tanks. Increasing the inductance and quality factor will also increase the distance over which the signal can be measured, which is essential for the practical use of this technology. The wireless EM device reported in Section III can also benefit from these changes. As indicated in (2), to increase inductance, the number of turns in a stentenna is one of the most important factors. In the test cases described here, this is limited because of the spatial resolution of the machining, which was performed by μEDM using a wire-tip as the cutting electrode. Batch mode μEDM [17] can achieve finer geometries because the cutting electrodes are lithographically fabricated on a microchip. This leads to more turns per unit length of the stentenna, which leads to higher inductance. (Batch mode μEDM also offers higher precision and about 100X improvement in throughput under the proper circumstances.) Another variable that affects the quality factor is parasitic resistance. The parasitic resistance of the stentennas can be reduced by coating them with a low-resistivity metal such as gold or copper as demonstrated in the wireless EM device. Stentennas that offer higher electrical performance will also contribute to achieve better coupling with external circuitry at the other end of the wireless link.

Another task that lies ahead is to evaluate the biological impact of the proposed structures in the context of various applications. Vascular applications, for example, may face challenges such as weakened arterial walls, clot formation, migration of the structure under certain physical conditions, etc. Further, if the structures must be coated with drug-eluting materials, the consequent changes in mechanical and electrical properties also must be investigated.

V. Conclusion

This effort has demonstrated, in a preliminary manner, the possibility of using steel structures that are micromachined from planar foil to monitor intraluminal pressure and flow. Of the approaches investigated, the first integrates micromachined capacitive pressure sensors with an inductive antenna stent. This structure retains compatibility with standard stenting tools and procedures, as demonstrated by its the deployment inside a mock artery using an angioplasty balloon. It can be used to monitor both pressure and flow of both insulating and conductive liquids, and is also suitable for air passages. However, the flow velocity is not measured directly, and must be deduced from the pressure. The second approach exploits an EM flow detection mechanism that can be applied to only polarizable liquids, including blood, and provides a more direct measurement of flow velocity that is less affected by the properties of the liquid. However, it does not provide pressure information. Its demonstration used a micromachined intraluminal cuff that included a pair of electrodes that were mechanically coupled but electrically isolated by dielectric links. It is anticipated that in the future, the use of high-resolution μEDM (with the help of lithographically patterned cutting tools) will allow more intricate patterns to be developed in such structures, allowing, for example, stentennas with higher inductance. In addition, the integration of this fabrication process with other planar technologies will facilitate the integration of elements such as pressure sensors and varactors.

Acknowledgment

The authors thank Dr. A. DeHennis for fabricating the capacitive pressure sensors and providing helpful advise regarding testing and calibration procedures. They also thank Dr. S. Mutlu for the parylene coating of samples.

References

[1] E. R. Edelman and C. Rogers, "Pathobiologic responses to stenting," *Amer. J. Cardiol.*, vol. 81, no. 7A, pp. 4E–6E, 1998.
[2] M. D. Addis, D. T. Baril, S. H. Ellozy, T. Jakobs, A. Carroccio, V. Teodorescu, and M. L. Marin, "Endovascular therapy for aortic disease," *Surg. Technol. Int.*, vol. 13, pp. 221–226, 2004.
[3] P. L. Faries, R. Dayal, J. Rhee, S. Trocciola, and K. C. Kent, "Stent graft treatment for abdominal aortic aneurysm repair: Recent developments in therapy," *Current Opin. Cardiol.*, vol. 19, no. 6, pp. 551–557, Nov. 2004.
[4] "Abdominal aortic aneurysms," *Physician's Week.*, vol. 1, no. 5, Apr. 2004.
[5] N. Al-Mubarak and S. S. Iyer, "Carotid artery stenting for the high surgical risk patients," *J. Cardiovasc. Surg.*, vol. 46, no. 1, pp. 1–8, Feb. 2005.
[6] S. N. Cullen and R. W. Chapman, "Review article: Current management of primary sclerosing cholangitis," *Alimentary Pharmacol. Therap.*, vol. 21, no. 8, pp. 933–948, Apr. 2005.
[7] K. E. Monkemuller, S. Kahl, and P. Malfertheiner, "Endoscopic therapy of chronic pancreatitis," *Digest. Diseases*, vol. 22, no. 3, pp. 280–291, 2004.
[8] Y. Saito and H. Imamura, "Airway stenting," *Surg. Today*, vol. 35, no. 4, pp. 265–270, 2005.
[9] R. L. Carrau, "Use of stents in head and neck surgery," *Current Opin. Otolaryngol. Head Neck Surg.*, vol. 13, no. 2, pp. 105–106, Apr. 2005.

[10] A. DeHennis and K. D. Wise, "A double-sided single-chip wireless pressure sensor," in *Proc. IEEE Int. Conf. Micro Electro Mechan. Syst. (MEMS)*, 2002, pp. 252–255.
[11] E. Park, J. Yoon, and E. Yoon, "Hermetically sealed inductor-capacitor (LC) resonator for remote pressure monitoring," *Japan. J. Appl. Phys.*, vol. 37, pp. 7124–7128, 1998.
[12] O. Akar, T. Akin, and K. Najafi, "A wireless batch sealed absolute capacitive pressure sensor," *Sens. Actuators A*, vol. 95, pp. 29–38, 2001.
[13] M. A. Fonseca, J. M. English, M. von Arx, and M. G. Allen, "Wireless micromachined ceramic pressure sensor for high-temperature applications," *J. Microelectromech. Syst.*, vol. 11, no. 4, pp. 337–343, Aug. 2002.
[14] A. DeHennis and K. D. Wise, "A fully-integrated multi-site pressure sensor for wireless arterial flow characterization," *J. Microelectromech. Syst.*, vol. 15, no. 3, pp. 678–685, Jun. 2006.
[15] S. Canic, K. Ravi-Chandar, Z. Krajcer, D. Mirkovic, and S. Lapin, "Mathematical model analysis of wallstent™ and AneuRx™: Dynamic responses of bare-metal endoprosthesis compared with those of stent-graft," *Texas Heart Inst. J.*, vol. 32, no. 4, pp. 502–506, 2005.
[16] K. Takahata and Y. B. Gianchandani, "A planar approach for manufacturing cardiac stents: Design, fabrication, and mechanical evaluation," *J. Microelectromech. Syst.*, vol. 13, no. 6, pp. 933–939, 2004.
[17] ——, "Batch mode microelectrodischarge machining," *J. Microelectromech. Syst.*, vol. 11, no. 2, pp. 102–110, 2002.
[18] K. Takahata, A. DeHennis, K. D. Wise, and Y. B. Gianchandani, "Stentenna: A micromachined antenna stent for wireless monitoring of implantable microsensors," in *Proc. IEEE Int. Conf. Eng. Med. Biol. Soc. (EMBS)*, 2003, pp. 3360–3363.
[19] ——, "A wireless microsensor for monitoring flow and pressure in a blood vessel utilizing a dual-inductor antenna stent and two pressure sensors," in *Proc. IEEE Int. Conf. Micro Electro Mech. Syst. (MEMS)*, 2004, pp. 216–219.
[20] K. Takahata and Y. B. Gianchandani, "A micromachined stainless steel cuff for electromagnetic measurement of flow in blood vessels," in *Proc. Solid-State Sensor and Actuator Workshop*, Hilton Head, SC, 2004, pp. 290–293.
[21] ——, "Micromachined intraluminal devices for active and passive electromagnetic measurements of flow," in *Proc. IEEE Int. Conf. Micro Electro Mech. Systems (MEMS)*, 2005, pp. 863–866.
[22] J. G. Webster, *The Measurement, Instrumentation, and Sensors Handbook*. Boca Raton, FL: CRC, 1999, vol. 28.6.
[23] H. J. Yoon, S. Y. Kim, S. W. Lee, and S. S. Yang, "Fabrication of a micro electromagnetic flow sensor for micro flow rate measurement," in *Proc. SPIE Symp. Smart Struc. Mat.*, 2000, pp. 264–271.
[24] D. F. Young, "Some factors affecting pressure-flow relationships for arterial stenoses," in *ASME Conf. Appl. Mech. Bioeng. Flu. Eng.*, 1983, pp. 87–90.
[25] J. C. Conti, E. R. Strope, L. M. Goldenberg, and K. S. Price, "The durability of silicone versus latex mock arteries," in *Proc. ISA Biomed. Sci. Instrum. Symp.*, 2001, vol. 37, pp. 305–312.
[26] A. B. Fontaine, K. Koelling, S. D. Passos, J. Cearlock, R. Hoffman, and D. G. Spigos, "Polymeric surface modifications of tantalum stents," *J. Endovasc. Surg.*, vol. 3, no. 3, pp. 276–283, 1996.
[27] P. D. Harvey, *Engineering Properties of Steel*. Metals Park, OH: American Society for Metals, 1999.
[28] MatWeb Automation Creations, Inc. [Online]. Available: http://www.matweb.com
[29] A. DeHennis and K. D. Wise, "An all-capacitive sensing chip for temperature, absolute pressure, and relative humidity," in *IEEE Int. Conf. Solid-State Sens., Actuators and Microsyst.(Transducers)*, 2003, pp. 1860–1863.
[30] Safety Level of Electromagnetic Radiation With Respect to Personnel IEEE, Amer. Nat. Standards Inst., 1974, ANSI C95.1-1974.
[31] A. Kolin, "An alternating field induction flow meter of high sensitivity," *Rev. Sci. Instrum.*, vol. 16, no. 5, pp. 109–116, 1945.
[32] F. Hofmann, *Fundamentals of Electromagnetic Flow Measurement*, Third ed. Brochure: Krohne Inc., 2003.
[33] B. H. Brown, R. H. Smallwood, D. C. Barber, P. V. Lawford, and D. R. Hose, *Medical Physics and Biomedical Engineering*. Bristol and Philadelphia: Inst. Physics, 1999, pp. 608–611.
[34] C. Roberts, *Blood Flow Measurement*. Baltimore, MD: Williams and Wilkins, 1972.
[35] A. Kolin, "A new approach to electromagnetic blood flow determination by means of catheter in an external magnetic field," *Proc. Nat. Acad. Sci.*, vol. 65, no. 3, pp. 521–527, 1970.
[36] C. J. Mills, "A catheter tip electromagnetic velocity probe," *Phys. Med. Biol*, vol. 11, no. 2, pp. 323–324, 1966.
[37] A. Kolin, "Approaches to blood-flow measurement by means of electromagnetic catheter flow meters," *IEEE Trans. Magn.*, vol. 6, pp. 308–314, Jun. 1970.
[38] ——, "An electromagnetic catheter blood flow meter of minimal lateral dimensions," *Proc. Nat. Acad. Sci.*, vol. 66, no. 1, pp. 53–56, May 1970.
[39] J. P. Biscar, "Three-Electrode probe for catheter-type blood flowmeters," *IEEE Trans. Biomed. Eng.*, vol. 20, pp. 62–63, Jan. 1973.
[40] D. M. Clark and D. G. Wyatt, "An improved perivascular electromagnetic flowmeter," *Med. Biolog. Eng.*, vol. 7, pp. 185–190, 1969.
[41] L. L. Chu, K. Takahata, P. Selvaganapathy, Y. B. Gianchandani, and J. L. Shohet, "A micromachined kelvin probe with integrated actuator for microfluidic and solid-state applications," *J. Microelectromech. Syst.*, vol. 7, pp. 691–698, Aug. 2005.
[42] J. A. Shercliff, *The Theory of Electromagnetic Flow-Measurement*. Cambridge Univ. Press, U.K.: Cambridge, 1962.

Kenichi Takahata (M'04) received the B.S. degree in physics from Sophia University, Tokyo, Japan, in 1990 and the M.S. and Ph.D. degrees in electrical engineering from the University of Michigan, Ann Arbor, in 2004 and 2005, respectively.

In 1990, he joined Matsushita Research Institute Tokyo, Inc. (Panasonic) and was with Matsushita Electric Industrial Co., Japan, until 2001. At Matsushita, he was engaged in research and development of micromechanics and microfabrication technologies including microelectrodischarge machining (μEDM) partially for the Japanese National Project "Micromachine Technology." In 1997, he was appointed Researcher in the International Joint Research Program supported by New Energy and Industrial Technology Development Organization (NEDO) of Japan, which explored the compatibility between μEDM and deep X-ray lithography (LIGA) processes at the University of Wisconsin, Madison. From 1999 through 2001, he held a Visiting Scientist position at the University of Wisconsin, Madison, where he investigated μEDM techniques that utilized lithographically fabricated electrodes. His doctoral research at the University of Michigan involved batch manufacturing technologies based on μEDM and application to MEMS with a focus on implantable devices and sensors. From 2005 to 2006, he was a Senior Research Engineer at 3M Company, St. Paul, MN. Presently, he is an Assistant Professor with the Department of Electrical and Computer Engineering, University of British Columbia, Vancouver, Canada. He currently has 25 publications, six issued patents, and 20 pending patents in the United States and Japan. His research interests are in MEMS realized by a combination of silicon and nonsilicon-based manufacturing technologies.

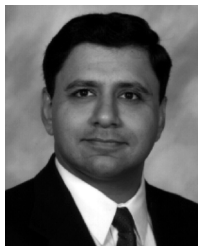

Yogesh B. Gianchandani (S'83–M'85–SM'04) received the B.S., M.S, and Ph.D. degrees in electrical engineering, with a focus on microelectronics and MEMS.

He is presently a Professor with the Department of Electrical Engineering and Computer Science and holds a joint appointment with the Department of Mechanical Engineering, University of Michigan, Ann Arbor. At the University of Michigan, he serves as the Director of the College of Engineering Interdisciplinary Professional Degree Program in Integrated Microsystems. Prior to this, he was with the Engineering and Computer Science Department, University of Wisconsin, Madison. He has also held industry positions with Xerox Corporation, Microchip Technology, and other companies, working in the area of integrated circuit design. His research interests include all aspects of design, fabrication, and packaging of micromachined sensors and actuators and their interface circuits. He has published about 150 papers in the field of MEMS, and has about 25 patents issued or pending.

Prof. Gianchandani is the recipient of a National Science Foundation Career Award. He serves on the editorial boards of IOP *Journal of Micromechanics and Microengineering* and *Journal of Semiconductor Technology and Science*, and served as a section editor for *Sensors and Actuators* for five years. He also served on the steering and technical program committees for the IEEE/ASME International Conference on Micro Electro Mechanical Systems (MEMS), and as a General Co-Chair for this meeting in 2002.

Kensall D. Wise (S'61–M'69–SM'83–F'86) received the B.S.E.E. degree with highest distinction from Purdue University, West Lafayette, IN, in 1963 and the M.S. and Ph.D. degrees in electrical engineering from Stanford University, Stanford, CA, in 1964 and 1969, respectively.

From 1963 to 1965 (on leave 1965–1969) and from 1972 to 1974, he was a Member of Technical Staff at Bell Telephone Laboratories, where his work was concerned with the exploratory development of integrated electronics for use in telephone communications. From 1965 to 1972, he was a Research Assistant and then a Research Associate and Lecturer with the Department of Electrical Engineering at Stanford University, working on the development of integrated circuit technology and its application to solid-state sensors. In 1974, he joined the Department of Electrical Engineering and Computer Science at the University of Michigan, Ann Arbor, where he is now the J. Reid and Polly Anderson Professor of Manufacturing Technology and Director of the NSF Engineering Research Center for Wireless Integrated MicroSystems. His present research interests focus on the development of integrated microsystems for health care, process control, and environmental monitoring.

Dr. Wise organized and served as the first chairman of the Technical Subcommittee on Solid-State Sensors of the IEEE Electron Devices Society (EDS). He was General Chairman of the 1984 IEEE Solid-State Sensor Conference, Technical Program Chairman of the IEEE International Conference on Solid-State Sensors and Actuators (1985), and IEEE-EDS National Lecturer (1986). He served as General Chairman of the 1997 IEEE International Conference on Solid-State Sensors and Actuators. He received the Paul Rappaport Award from the EDS (1990), a Distinguished Faculty Achievement Award from the University of Michigan (1995), the Columbus Prize from the Christopher Columbus Fellowship Foundation (1996), the SRC Aristotle Award (1997), and the 1999 IEEE Solid-State Circuits Field Award. In 2002, he was named the William Gould Dow Distinguished University Professor at the University of Michigan. He is a Fellow of the AIMBE and a member of the United States National Academy of Engineering.